Direct 3D Printing of Optical Elements with Xolography

Martin Herder, Yves Garmshausen, Marvin-Pascal C. Tauber, Yousef Arzhangnia, Marcus Reuter
xolo GmbH, Volmerstr. 9b, 12489 Berlin, Germany

ABSTRACT

Xolography is a volumetric 3D printing method utilizing dual-color photoinitiators to fabricate layer-free objects from photopolymer resins, ranging from millimeters to centimeters in size. It enables fast, continuous printing of complex three-dimensional objects, which are free of internal interfaces and possess optical-grade surfaces immediately after printing. The development of photobleaching dual-color photoinitiators together with a light sheet configuration, which prevents the evolution of striping artifacts, allows us to 3D print transparent and smooth optical elements within few minutes printing time and without the need for any additional process steps such as coating or polishing. In combination with its capability to print complex freeform geometries and the use of highly viscous photopolymer resins, Xolography has the potential to revolutionize prototyping and fabrication of optical elements

Keywords: Xolography, Volumetric Additive Manufacturing, 3D Printing, Optical Elements

1. INTRODUCTION

The demand for high-precision optics in technological fields, such as sensors, medical devices and AR/VR technologies, has exposed the limitations of current additive manufacturing (AM) methods for producing optical elements.[1] While only photopolymerization-based 3D printing offers the high resolution needed for printing of optics, currently available methods have significant drawbacks in terms of object size, fabrication speed, or surface quality.

Stereolithography (SLA) and Digital Light Processing (DLP) show pronounced staircase effects on the surface as well as internal interfaces in the bulk of printed parts due to the layer-wise printing process (Figure 1a). In order to attain optically smooth surfaces, additional postprocessing steps on the printed parts such as coating or polishing are required.[2,3] Inkjet printing (Figure 1b) is an industrially scalable fabrication process for optical elements,[4] but it is restricted to the use of low-viscosity materials and mostly produces 2.5D structures rather than real three-dimensional objects. This limits the material performance and durability as well as its applicability for complex optical designs. In contrast, Two-Photon Polymerization (2PP) offers unmatched geometrical freedom and print resolution allowing the fabrication of complex miniature optics possessing optical grade surfaces (Figure 1c).[5,6] However, for larger objects in the millimeter to centimeter scale, this method is sincerely limited by long fabrication times and high costs.

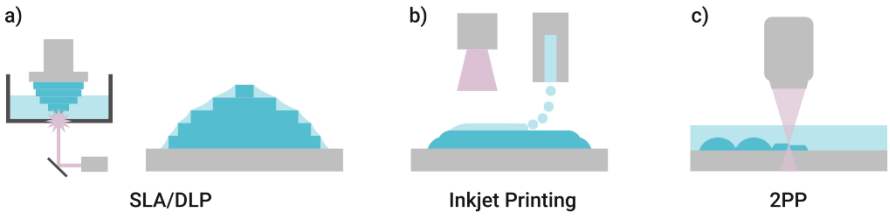

Figure 1. Illustration of state-of-the-art methods for 3D printing of optical elements: a) SLA and DLP require additional process steps such as coating of the final part for generating optically smooth surfaces. b) Inkjet Printing is restricted to low-viscosity materials and mostly applicable for 2.5D geometries. c) 2PP enables high precision and high-resolution prints but larger objects need excessively long fabrication times.

With Xolography, a novel volumetric additive manufacturing (VAM) technology, complex three-dimensional parts ranging from millimeters to centimeters in size are fabricated within seconds using viscous photocurable polymer materials.[7,8,9] Ultra-fast fabrication speeds of up to 24 mm min^{-1} along print direction can be realized.[10] Its volumetric working principle fully omits the use of a build platform or support structures attached to the object, thus granting almost full geometrical freedom to the object designer. Most importantly, Xolography is a continuous printing process resulting in layer-free objects, avoiding staircase effects and internal interfaces. The printed parts possess homogeneous bulk

Advanced Fabrication Technologies for Micro/Nano Optics and Photonics XVIII, edited by
Christophe Moser, Eva Blasco, Debashis Chanda, Proc. of SPIE Vol. 13381,
133810C · © 2025 SPIE · 0277-786X · doi: 10.1117/12.3039464

properties and optically smooth surfaces directly out of the printer, eliminating the need for additional process steps. This makes Xolography particularly suited for the additive prototyping and fabrication of optical elements.[11]

Based on our recent advances, i.e. full bleaching of photoinitiator molecules and artifact-free printing, here we report on direct printing of a diverse range of smooth optical elements on the multiple millimeter scale, showing the capability of Xolography to fabricate optical components with geometrical freedom and ease of processing.

2. METHODS

Working principle of Xolography

Xolography is based on a transparent container filled with a viscous photopolymer, which is continuously moving through a thin UV light sheet (Figure 2, left). During that movement, a visible light projection is focused from a 90 degree angle onto the light sheet plane within the photopolymer container. Hardening of the photopolymer is induced only in regions, where both the UV *and* visible light intersect at the same time. Eventually, the desired object appears floating within the volume of the resin.

The technology relies on the presence of a dual-color photoinitiator (DCPI) within the polymer resin, which imparts its synergistic curing with light of two different wavelengths λ_1 and λ_2 (Figure 2, right): In contrast to a conventional photoinitator, which reacts with just one wavelength of light, e.g. UV light (λ_1), to start the polymerization, the DCPI does not yet form an initiating species upon absorption of a UV photon. Instead, the molecule is transformed from its dormant form A to the active form B by UV excitation. While form B does not start the polymerization yet, it possesses a broad absorption band in the visible region, thus absorbing visible light (λ_2) coming from the projection unit. Upon excitation of form B with visible light (λ_2), the initiating species C, typically a radical, is produced and polymerization starts. Importantly, active form B is metastable and quickly reverts back to the dormant form A in the absence of irradiation. This makes sure that visible light absorption is immediately depleted when the UV light has passed a certain volume element, avoiding curing in volume elements behind the light sheet.

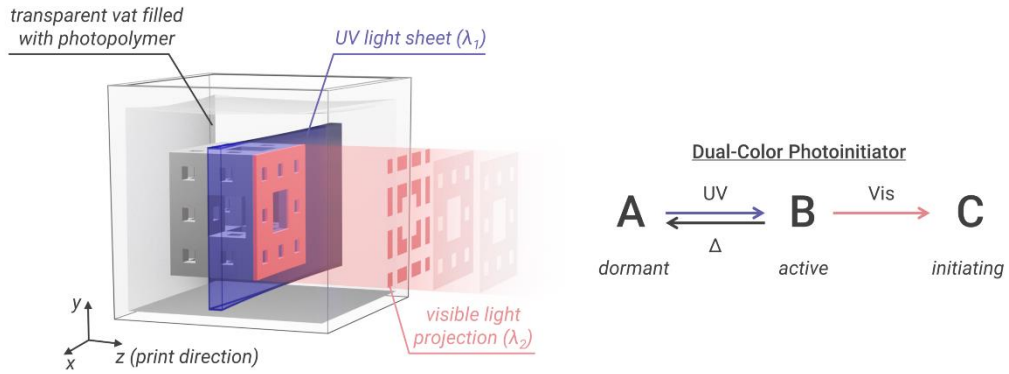

Figure 2. Working principles of Xolography and dual-color photoinitiators (DCPIs).

Print hardware

For the volumetric printing of optical elements, xolo's commercial *XUBE-2* hardware[12] is used consisting of a light sheet module (LSM), a projection unit (PU), and a cuvette holder. The PU and the cuvette holder are moved along linear axes during the printing process. The LSM is equipped with two laser diodes emitting at 375 nm (λ_1). Using rotating mirrors the light sheet is generated from both sides of the build room and is aligned in the x-y-plane (see Figure 2 for the reference coordinate system). Low-NA optics are used for focusing the light sheet in the z-dimension resulting in a thickness of 50 µm FWHM in the center of the cuvette with a thickness variation of less than 10% along the x-axis.

The PU is equipped with a high-power RGB LED unit as light source, a DMD chip with 4K resolution and projection optics for focusing the projected image onto the light sheet plane within the build room. The size of the projected image is adapted to the build room in use. Here, standard 10x35x10 mm³ UV-Vis cuvettes having four transparent windows are

used, setting the lateral projection size to 10.0×17.8 mm². The emission of the projection unit does not contain any wavelengths below 450 nm.

The movement of the linear axes, the adjustment of UV and Vis light intensity as well as the video signal fed into the projection unit are controlled by xolo's proprietary print software *xolid*.

Material

The urethane methacrylate-based material *xoloClear* with a dynamic shear viscosity of $\eta = 2.5$ Pa s is used for printing of optical elements.[12] *xoloClear* contains the dual-color photointiator *DCPI 2001*, being reactive to a UV wavelength of $\lambda_1 = 375$ nm and visible wavelengths between $\lambda_2 = 450$-700 nm. The material is filled into 10×35×10 mm³ disposable fluorescence cuvettes having four transparent windows (BRAND GmbH) serving as resin container. Cuvettes are sealed via thermal lamination with polyamide foil and centrifuged in order to remove any remaining air bubbles before use.

Print process and workup

STL model files are loaded into the device software *xolid* and sliced with a layer thickness of 1 µm to generate a video to be played by the PU during the print. Print parameters (UV energy $E_{UV} = 12$ mJ mm^{-2} and print speed $v_p = 2$ mm min^{-1}) are set within the software, the resin-filled cuvette is placed into the cuvette holder and the print is started.

After the print has finished, the cuvette is taken out and opened in order to remove the printed object from the non-polymerized resin using tweezers or a wire hook. It is consecutively washed in stirred baths of tripropyleneglycol monomethylether (TPM, AprintaPro GmbH) for 5 min, ethanol (96%, SigmaAldrich) for 30 s, and ethanol containing 1 wt% of TPO-L (TCI Chemicals) for 2 min. Then, it is dried in a ventilated oven at 80°C and postcured under vacuum or argon atmosphere in a UV-LED chamber (Rapidshape RSCure) for 5 min. An optional thermal annealing step is performed in a ventilated oven at 110°C for 15 min. Bleaching of residual color is performed on the already postcured parts by placing them under a white light LED array (color temperature 6000 K, 130 mW/cm²) for 15 min.

Analytical methods

UVVis spectroscopy is performed on a Cary 50 UVVis spectrophotometer (Varian) equipped with a Luma 4 cuvette holder (Quantum Northwest Inc.) having open windows on all four sides of the cuvette. Disposable semimicro cuvettes (BRAND GmbH) are used and samples are temperature equilibrated at 25 °C for 10 min prior to measurement. For baseline measurements ethyl acetate solvent is used. While recording absorbance spectra, resin samples are irradiated within the cuvette holder using collimated UV and Vis LEDs (Thorlabs Inc.). Output power of the LEDs is measured using a Thorlabs PM400 powermeter equipped with a S130C photodiode sensor.

Printed objects are photographed using a standard digital camera and an Andonstar AD409 Pro Digital Microscope. Shape and surface roughness measurements are performed on a Keyence VK-X3050 3D laser confocal microscope equipped with Nikon CF IC EPI Plan objectives ELWD 20X (NA 0.4), ELWD 50X (NA 0.55) and 50X (NA 0.80). Surface roughness is calculated using multi-line profiles (n = 6) and a cutoff wavelength of $\lambda_c = 0.08$ mm.

3. RESULTS AND DISCUSSION

Dual-color photopolymerization

At the core of Xolography volumetric printing is the dual-color-photoinitiator (DCPI), enabling selective curing of arbitrary volume elements within the build room by intersecting light beams of two different wavelengths. *xoloClear* material utilized in this work contains the *DCPI 2001*, which is a spiropyran-based photoswitch[13] (Figure 3a) undergoing type II photoinitiation together with a tertiary amine co-initiator upon simultaneous excitation with UV (λ_1, 375 nm) and visible light (λ_2, 450 – 700 nm). The spiropyran (SP) form of the DCPI only absorbs UV wavelengths with its absorbance onset being in the range of λ_1 (Figure 3b). Upon excitation with UV light the SP form ring-opens into the metastable merocyanine (MC) form, which possesses a broad absorption band in the visible region. The MC form is short-lived with a half-life of 3.0 s in the viscous resin matrix, thermally reverting back to the SP form in the absence of light (Figure 3c). This ensures

that the visible light projected into the resin container is only absorbed within volume elements momentarily exposed to the UV light sheet, while in regions, where the light sheet has already passed, the Vis light absorbance is quickly depleted.

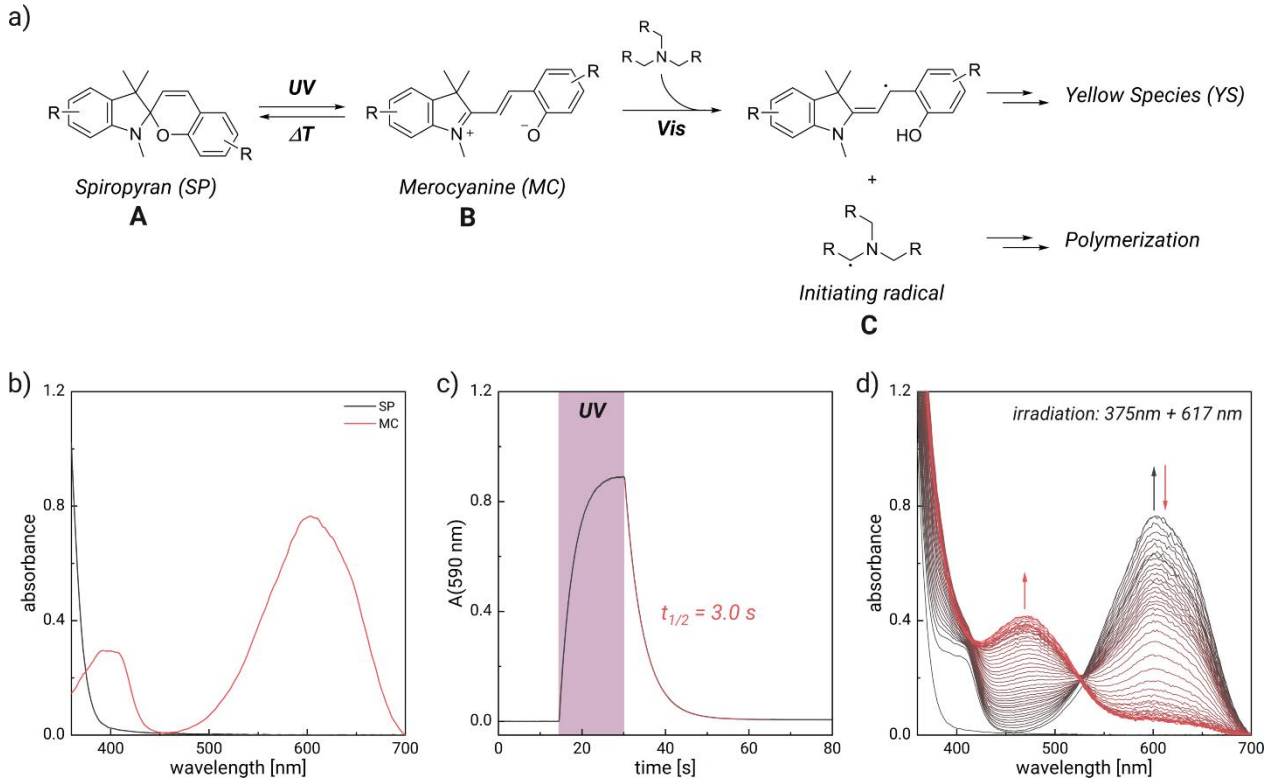

Figure 3. a) Reaction of a spiropyran-based dual-color-photoinitiator (DCPI) upon activation with UV and visible light. b) UVVis absorbance spectra of the SP and MC forms of *DCPI 2001* in urethane methacrylate resin. c) Fast MC absorbance decay after stopping UV irradiation. d) UVVis spectra recorded during irradiation of *DCPI 2001* with UV (375 nm LED, 14 mW/cm²) and visible light (617 nm LED, 42 mW/cm²) in urethane methacrylate resin containing co-initiator. Time gap between individual spectra is 6 s. Scattering induced by resin hardening during the experiment was corrected for by subtracting a constant baseline value recorded at λ = 700 nm. At early stages of irradiation, the broad absorption band centered at 600 nm is quickly formed corresponding to the MC form. Upon continuing dual-color irradiation, the MC band slowly depletes while a band centered at 490 nm evolves, indicative of the formation of the YS.

When the metastable MC form is excited by a Vis light photon, it undergoes photoelectron transfer with the tertiary amine co-initiator resulting in the formation of two radicals (Figure 3a): One radical is situated on the ring-opened DCPI molecule while the other radical is situated on the amine co-initiator molecule. The latter radical is of high reactivity, thus initiating the polymerization by reacting with (meth)acrylate monomer or oligomer, which eventually leads to local cross-linking and hardening of the matrix. The radical situated on the DCPI molecule is of significantly lower reactivity and presumably is not able to initiate the polymerization reaction. It undergoes different follow-up reactions, such as radical recombination or disproportionation with a chain end, which eventually leads to the formation of a colored species. The latter we denote "Yellow Species" (YS), as it causes a typical yellow-orange color of printed objects. During a dual-color polymerization experiment, the depletion of the MC absorbance centered at 600 nm and the evolution of the YS with its band centered at 490 nm can be monitored by UVVis spectroscopy using in-situ irradiation with UV and Vis light (Figure 3d).

The formation of the YS hampers the utility of dual-color polymerization for 3D printing transparent and colorless objects. Nevertheless, by structural modification of the DCPI molecular motifs, it is possible to induce further photoreactivity to the YS, allowing full bleaching of printed parts during postcuring processes. This is the case for *DCPI 2001*, which we utilize in optics printing reported here.

DCPI bleaching during postprocessing

Directly after print, solidified objects within the resin container possess a shallow orange color due to the presence of the YS. The color remains during washing and postcuring in a UV LED chamber, as remaining *DCPI 2001* is converted into initiating radicals and YS. Notably, the evolution of color at that stage is limited to a shallow orange (Figure 4a, left), as most of the YS is already bleached during UV postcuring. Upon placing the printed and postcured object under a white light LED for a further 15 min, the remaining color disappears, leaving behind a transparent and colorless lens object (Figure 4a, right).

Bleaching of YS can be followed by UVVis spectroscopy using in-situ irradiation. After performing dual-color polymerization of the sample using UV and Vis light LEDs (compare Figure 3d) the remaining absorption band centered at 490 nm is depleted using 455 nm irradiation (Figure 4b).

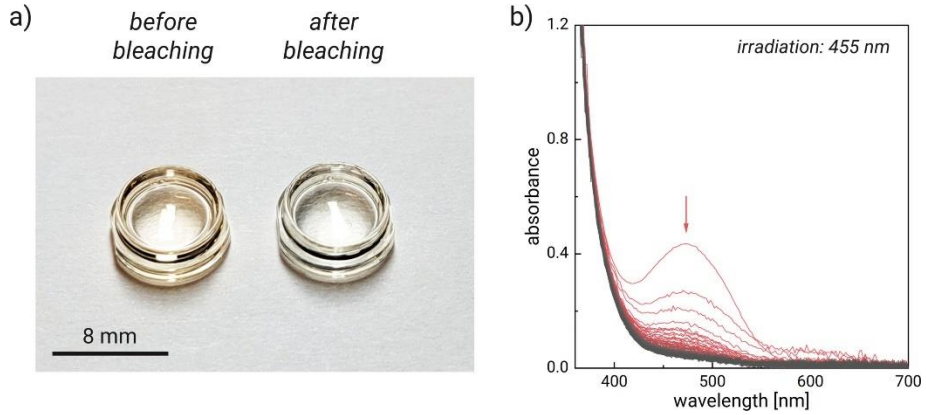

Figure 4. a) Optical photograph of printed lenses directly after UV and thermal postcure (left) and after subsequent bleaching (right) using white light LED array (6000 K, 130 mW/cm², 15 min). b) UVVis spectra recorded during bleaching of *DCPI 2001* in polymerized urethane methacrylate resin using 455 nm LED light (350 mW/cm²). Time gap between individual spectra is 6 s.

Avoiding striping artifacts

Striping artifacts are commonly known in light sheet-based fluorescence microscopy, deteriorating the quality of recorded images.[14] Similarly, for VAM methods such as Computed Axial Lithography (CAL) striping artifacts are reported to deteriorate the printed object's internal homogeneity and surfaces, eventually making them appear opaque.[15] In VAM, light has to travel deep into the resin container in order to induce photopolymerization. Thus, any particulate matter, such as dust or small air bubbles, can lead to pronounced local shadowing of the regions directly behind. Additionally, in case of coherent lasers used as source of illumination, interference effects (laser speckle) can lead to local intensity fluctuations, which are translated into small refractive index (RI) variations of the just-cured photopolymer. Due to self-focusing effects the initially small RI variations are aggravated into the bulk of the cured object in the form of periodic stripes or ripples.

In Xolography, the UV light sheet is generated using laser diodes, which, in a simple optical configuration of the LSM, lead to marked striping artifacts. They are recognized as horizontal ripples within the printed parts oriented along the extension direction of the light sheet, i.e. the x-axis of the build room (Figure 5a,b,d). Obviously, these artifacts significantly deteriorate the transparency and smoothness of printed parts.

In order to avoid striping artifacts, we modified the optical setup of the LSM in a way to increase the angular diversity of light beams travelling through the UV light sheet plane. Thus, phase correlation between individual laser beams is effectively destroyed and shadowing effects by air bubbles and particles are reduced. As a result, printed objects appear homogeneous and smooth without compromising lateral and axial resolution (Figure 5c,e).

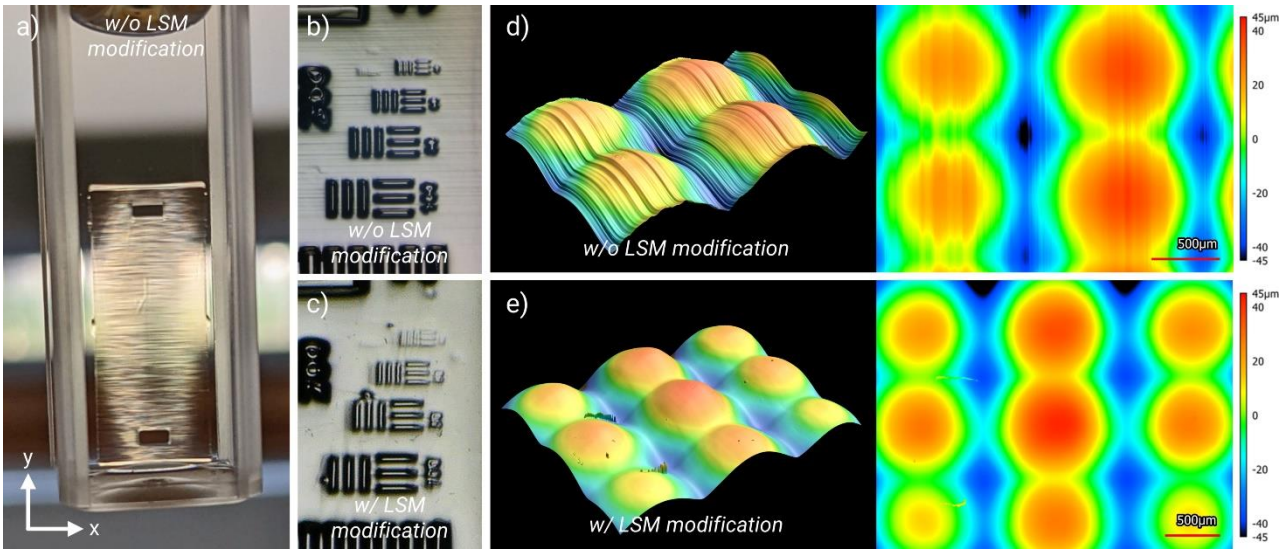

Figure 5. Removal of striping artifacts. a) Optical photograph of a 10 mm sized cuvette containing a flat rectangular plate printed without modification of the light sheet module (LSM) showing pronounced ripples. Arrows indicate orientation of the object within the printer. b)-c) Microscope images of printed resolution target without and with LSM modification, respectively. d)-e) Height profile of a microlens array printed without and with LSM modification, respectively, as measured by laser confocal microscopy.

Optical lens printing

Figure 6 shows a collection of mm-sized lenses and microlens arrays, which are printed using *xoloClear* material within the 10×17.8×10 mm³ build room. In all cases printing direction (z) was normal to the shown surface plane. The print time of individual objects indicated below the picture correlates with their height at the utilized printing speed of 2 mm min^{-1}.

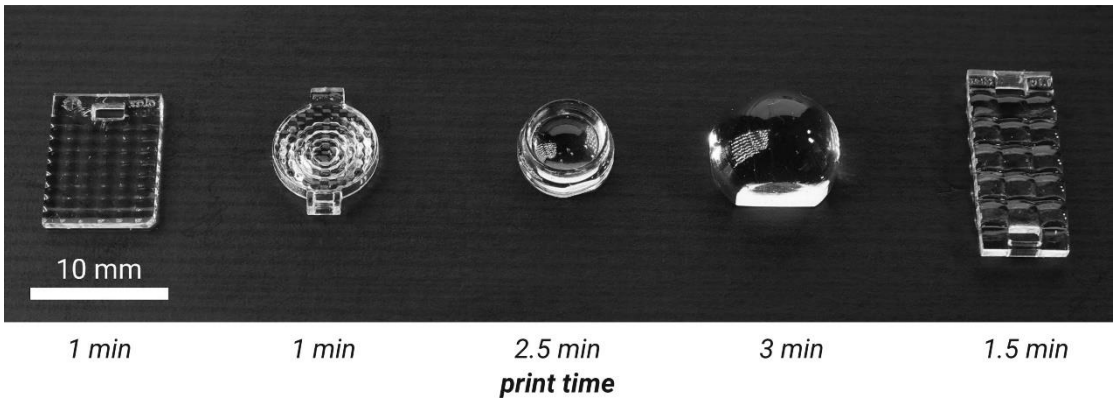

Figure 6. Photograph of a collection of printed lenses. From left to right: Plano-convex square grid microlens array (adapted from Thorlabs Inc, part number: MLA1[16]), diffusor lens with microprism array (in-house design), biconvex lens in a frame (in-house design), aspheric condenser lens (adapted from Thorlabs Inc., part number: ACL108U[17]), plano-convex microlens array with toric lenslets (in-house design). Printing times for the individual components are given below the image. All lenses were printed, washed, dried in air and postcured in a UV-chamber before the picture was taken.

The collection demonstrates Xolography's capability to fabricate simple and complex optical elements with ultra-short process times, as compared to other AM technologies (vide supra). Xolography's ability to produce versatile geometries with smooth surfaces straight from the printer is clearly visible to the naked eye. Apart from washing and postcuring, no additional process steps such as coating or polishing are required. Smooth surfaces are obtained in any direction, allowing to fabricate lenses with optical functions on their front and back sides, i.e. a diffusing microprism array with a Fresnel lens

on its back side (Figure 6, second from left) and a biconvex lens with different focal lengths on the front and back sides (Figure 6, third from left).

Lens characterization

In order to test the precision and reproducibility of the optical lens printing process, we printed six identical plano-convex lenses, which were adapted from a commercial lens item (Edmund Optics, part no. #32-471)[18]. After printing (print time 2 min at 2 mm min^{-1} print speed), the objects were washed in solvent, dried, postcured and bleached according to the procedure described in the Methods section. With the naked eye, the printed lenses are almost indistinguishable from the commercial part and they appear hard, colorless, and smooth (Figure 7a,b). Measuring surface roughness of printed lenses reveals values in the same range as the commercial lens, with Ra between 20-23 nm (Figure 7c, Table 1).

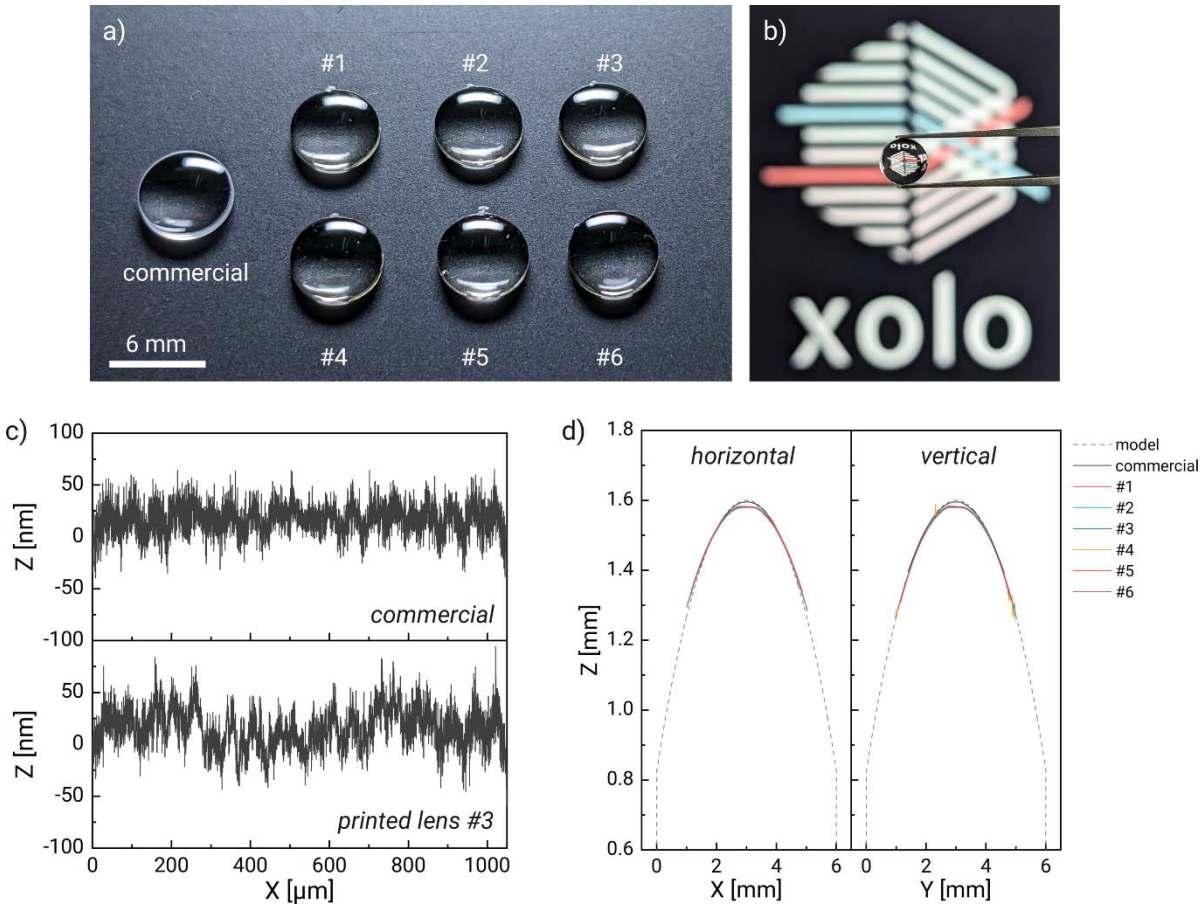

Figure 7. a) Photograph of six printed plano-convex lenses (diameter 6.0 mm, focal length 12 mm) and its commercial counterpart[13]. b) xolo's company logo imaged through one of the printed lenses. c) Comparison of measured surface roughness profiles (λ_c = 0.08 mm) obtained by laser confocal microscopy of the commercial and printed lenses. d) Comparison of front side curvature measured in horizontal and vertical orientation by laser confocal microscopy of printed lenses with the commercial lens and the input STL model.

For improved handling of printed lenses without having to touch the optical surfaces, a small hook was attached to the top of the printed lens, which was cut away after washing. Besides that, there were no modifications of the input geometry of the plano-convex lens, in particular no optimization, geometrical calibration or compensation procedures were employed in this experiment. Shape measurements reveal a small deviation of printed parts from the target geometry, which can be described as flattening of the radius of curvature (ROC) towards the center of the lens (Figure 7d). Over the sample size of six lenses, this shape deviation remains constant. Note that due to the highly reflective surface of printed lenses, laser confocal microscopy can only scan part of the curved lens face. More detailed investigations on the shape, waviness and surface roughness of printed optical elements are currently ongoing.

Table 1. Shape and surface roughness parameters of printed lenses measured with laser confocal microscopy.

	STL input	commercial lens	printed lenses						
			#1	#2	#3	#4	#5	#6	average
diameter [mm]	6.00	5.98	5.76	5.72	5.73	5.77	5.81	5.78	5.76 ± 0.03
ROC_{horiz} [mm]	6.2	6.6	7.1	7.1	7.0	7.1	7.2	7.0	7.1 ± 0.1
ROC_{vert} [mm]	6.2	6.5	6.6	6.6	6.5	6.4	6.4	6.6	6.5 ± 0.1
Ra [nm]		19	23	20	21	22	22	20	21 ± 1
Rq [nm]		23	27	23	25	28	27	24	26 ± 2
Rz [nm]		80	109	79	97	131	114	97	105 ± 16

4. CONCLUSION

Xolography, as volumetric 3D printing technique, advances the additive manufacturing of optical and microoptical elements by enabling the printing of geometrically complex parts with smooth surfaces directly from the printer. We show two key achievements towards printing of functional optical elements: imparting transparency to printed parts by photobleaching a colored by-product of the dual-color photoinitiator as well as avoiding striping artifacts commonly observed in volumetric 3D printing by inducing angular diversity within the UV light sheet. Together with a dedicated material *xoloClear*, we demonstrate the rapid fabrication of a diverse range of optical lenses and lens arrays up to 10x17 x10mm^3 size. Surface roughness of as-printed lenses is found to be in the range of commercially available parts. Our ongoing efforts concentrate on fine-tuning shape fidelity as well as making larger build rooms available for printing of optical elements.

By overcoming the limitations of conventional layer-based 3D printing methods and achieving unprecedented fabrication speeds, Xolography has the potential to revolutionize optics prototyping and manufacturing. Through collaborative research, we will further explore and refine its capabilities for fabricating optical and photonic devices.

5. REFERENCES

[1] Chekkaramkodi, D., Jacob, L., Shebeeb C M., Umer, R. and Butt, H., "Review of vat photopolymerization 3D printing of photonic devices", Addit. Manuf. 86, 104189 (2024). http://doi.org/10.1016/j.addma.2024.104189

[2] Berglund, G.D. and Tkaczyk, T.S., "Fabrication of optical components using a consumer-grade lithographic printer", Opt. Express 27, 30405-30420 (2019). http://doi.org/10.1364/OE.27.030405

[3] Chen, X., Liu, W., Dong, B., Lee, J., Ware, H.O.T., Zhang, H.F. and Sun, C., "High-Speed 3D Printing of Millimeter-Size Customized Aspheric Imaging Lenses with Sub 7 nm Surface Roughness", Adv. Mater. 30, 1705683 (2018). http://doi.org/10.1002/adma.201705683

[4] Beckert, E., Kemper, F., Schreiber, P., Reif, M., Dannberg, P. and Sauva, S., "Inkjet printing of microlens arrays on large, lithographic structured substrates", Proc. SPIE 10930, Advanced Fabrication Technologies for Micro/Nano Optics and Photonics XII, 109300C (4 March 2019). http://doi.org/10.1117/12.2507605

[5] Ristok, S., Thiele, S., Toulouse, A., Herkommer, A.M. and Giessen, H., "Stitching-free 3D printing of millimeter-sized highly transparent spherical and aspherical optical components", Opt. Mater. Express 10, 2370-2378 (2020). http://doi.org/10.1364/OME.401724

[6] Stender, B., Hilbert, F., Dupuis, Y., Krupp, A., Mantei, W. and Houbertz, R., "Manufacturing strategies for scalable high-precision 3D printing of structures from the micro to the macro range", Adv. Opt. Technol. 8, 225-231 (2019). https://doi.org/10.1515/aot-2019-0022

[7] Regehly, M., Garmshausen, Y., Reuter, M., König, N.F., Israel, E., Kelly, D.P., Chou, C.-Y., Koch, K., Asfari, B. and Hecht, S., "Xolography for linear volumetric 3D printing", Nature 588, 620–624 (2020). http://doi.org/10.1038/s41586-020-3029-7

[8] Stüwe, L., Geiger, M., Röllgen, F., Heinze, T., Reuter, M., Wessling, M., Hecht, S. and Linkhorst, J., "Continuous Volumetric 3D Printing: Xolography in Flow", Adv. Mater. 36, 2306716 (2024). http://doi.org/10.1002/adma.202306716

[9] Corrigan, N., Li, X., Zhang, J. and Boyer, C., "Xolography for the Production of Polymeric Multimaterials", Adv. Mater. Technol. 9, 2400162 (2024). http://doi.org/10.1002/admt.202400162
[10] König, N.F., Reuter, M., Reuß, M. et al., "Xolography for 3D Printing in Microgravity", Adv. Mater., 2413391 (2024). https://doi.org/10.1002/adma.202413391
[11] Herder, M. and Kuehr, S., "Direct 3D Printing of Smooth Optical Elements", Proc. SPIE 13205, 1320507-1 (2024). https://doi.org/10.1117/12.3034035
[12] xolo GmbH, Berlin, Germany, https://www.xolo3d.com/
[13] Drichel, A., Garmshausen, Y. and Hecht, S., Angew. Chem. Int. Ed., e202419531 (2025). https://doi.org/10.1002/anie.202419531
[14] Ricci, P., Gavryusev, V., Müllenbroich, C., Turrini, L., de Vito, G., Silvestri, L., Sancataldo, G. and Pavone, F.S., "Removing striping artifacts in light-sheet fluorescence microscopy: a review", Prog. Biophys. Mol. Biol. 168, 52-65 (2022). https://doi.org/10.1016/j.pbiomolbio.2021.07.003
[15] Rackson, C.M., Toombs, J.T., De Beer, M.P., Cook, C.C., Shusteff, M., Taylor, H.K. and McLeod, R.R., "Latent image volumetric additive manufacturing," Opt. Lett. 47, 1279-1282 (2022). https://doi.org/10.1364/OL.449220
[16] https://www.thorlabs.com/thorproduct.cfm?partnumber=MLA1
[17] https://www.thorlabs.com/thorproduct.cfm?partnumber=ACL108U
[18] https://www.edmundoptics.com/p/60mm-dia-x-120mm-fl-uncoated-plano-convex-lens/2356/